Heartfelt Face Perception via the Interoceptive Pathway – a MEG study

Jaejoong Kim[1], Hyeong-Dong Park[2], Ko Woon Kim[1,3], Dong Woo Shin[1], Sanghyun Lim[4], Hyukchan Kwon[4], Min-Young Kim[4], Kiwoong Kim[4], Bumseok Jeong[1]

[1]Computational Affective Neuroscience and Development Laboratory, KAIST, Graduate School of Medical Science and Engineering, Daejeon, Korea; KAIST Institute for Health Science and Technology, KAIST, Daejeon, Korea; [2]Laboratory of Cognitive Neuroscience, Center for Neuroprosthetics and Brain Mind Institute, Ecole Polytechnique Fédérale de Lausanne (EPFL), 9 Chemin des Mines, 1202 Geneva, Switzerland; [3]Department of Neurology, Chonbuk National University Hospital, Chonbuk National University Medical school, JeonJu, Korea; [4]Center for Biosignals, Korea Research Institute of Standards and Science, Daejeon, South Korea

Abstract

The somatic marker hypothesis proposes that cortical representation of visceral signals is a crucial component of emotion processing. There has been no previous study investigating the causal relationship among brain regions of visceral information processing during emotional perception. In this magnetoencephalography study of 32 healthy subjects, heartbeat evoked potential (HEP), which reflects cortical processing of heartbeats, was modulated by the perception of sad faces, but not other faces and text-based emoticons. We here provide the first evidence for an increased causal flow of heartbeat information from the right posterior insula to the anterior insula to the anterior cingulate cortex and from the right globus pallidus to the prefrontal cortices by sad faces. Moreover, this effect was not an effect of visual evoked potential, which indicates separate systems of interoceptive and visual processing. These findings provide important progress in the understanding of brain-body interaction during emotion processing.

Introduction

According to the James-Lange theory and the somatic marker hypothesis, emotional feelings are the mental experience of bodily states (A. Damasio & Carvalho, 2013; James, 1884). More specifically, emotional stimuli usually induce a change of bodily status (Williams et al., 2005). Then various feelings subsequently emerge from the perception of bodily status including a sense of viscera (A. Damasio & Carvalho, 2013). Many previous studies showed evidence of emotional stimulus-evoked somatic response. For example, a fearful stimulus enhances sympathetic responses like heart rate elevation and skin conductance modulation (Critchley et al., 2005; Williams et al., 2005), and a disgusting stimulus induces tachygastria (Harrison, Gray, Gianaros, & Critchley, 2010). Moreover, neuroimaging studies using fMRI or EEG have shown that generation of bodily responses by an emotional stimulus is related to activation of subcortical regions like the amygdala and hypothalamus (A. R. Damasio et al., 2000). On the other hand, there is rare evidence that supports a change of cortical interoceptive processing in the brain while experiencing emotional feeling. Given that signal of internal organs are cannot be identifiable without explicit measuring devices like electrocardiogram (ECG), it is difficult to investigate which brain activity was directly evoked by interoceptive signals. Thus, previous studies explored changes in the interoceptive processing during just the experience of emotional states and reported their relation with the anterior insula and anterior cingulate cortex (Adolfi et al., 2016; Critchley et al., 2005).

Heartbeat evoked potential (HEP), which is obtained by averaging electrophysiological signals time-locked to heartbeats, has been reported to be associated with the perception of heartbeat (Pollatos & Schandry, 2004), pain (Shao, Shen, Wilder-Smith, & Li, 2011), and feeling empathy (Fukushima, Terasawa, & Umeda, 2011). Moreover, HEP amplitude is attenuated in mood-related psychiatric disorders, including depression (Terhaar, Viola, Bär, & Debener, 2012)

and borderline personality disorder (Müller et al., 2015), suggesting a potential link between HEP and aberrant emotional processing.

Based on these theories and indirect evidence, we hypothesized that HEP would be associated with the feeling of emotional stimuli and would be modulated during perception of emotional expression such as face and emoticon. And the modulation effect would be different between positive and negative valences.

To test this idea, we used emotional faces and emotional emoticons that convey text-based emotion to evoke emotional feeling while measuring the HEP with magnetoencephalography (MEG). To verify the precise source of HEP modulation, T1-weighted structural magnetic resonance imaging (MRI) was acquired from all subjects. Importantly, we applied Granger causality analysis (Barnett & Seth, 2014) on sources to identify information flow between sources of HEP modulation.

We formulated the following specific hypotheses. First, we expected that HEP would be modulated by the emotional expression and this effect would appear in different spatiotemporal dynamics between emotional and neutral stimulus presentation. Second, the modulation of HEP by emotional expression would be localized in the previously known interoceptive region like the anterior/posterior insula and the anterior cingulate cortex in source level analysis. Third, we expected that information flow between these interoceptive regions would be modulated by emotional expression. To be more specific, we expected that bottom up heartbeat information processing starting from the posterior insula, which is the primary interoceptive sensory cortex (Barrett & Simmons, 2015), to the anterior insula would be enhanced by emotional expression, which is the pathway of generating emotional feeling predicted by the somatic marker hypothesis (A. Damasio & Carvalho, 2013). Finally, we hypothesized that neural activity that are evoked by heartbeat would have different spatiotemporal patterns compared to visual

evoked cortical activity. That is, we expected that locking the MEG signals by the cardiac signal would make the visual evoked effect disappear and vice versa.

Methods

Participants

Forty healthy participants (19 females, mean age of 24.03 ± 3.28 years) volunteered in the experiment. The expected effect sizes were not known in advance, so we chose a sample size of approximately 40 participants which was approximately two times more than those of previous MEG and EEG studies of HEP (Babo-Rebelo, Richter, & Tallon-Baudry, 2016; Fukushima et al., 2011; H.-D. Park, Correia, Ducorps, & Tallon-Baudry, 2014). All subjects had no neurological or psychological disease. MEG recording consisting of 4 runs was completed with one visit. High resolution T1 weighted MRI scans were acquired at another visit. In this MRI session, all subjects performed both functional MRI experiments consisting of emotion discrimination (unpublished) and/or decision (unpublished) tasks, and other structural MRIs such as diffusion tensor imaging (unpublished). Among forty subjects, we failed to acquire MEG data for five subjects due to magnetic field instability. Another three subjects were excluded in analysis because their ECG data were too noisy or absent. Therefore, thirty-two subjects were included for further analysis. All participants submitted written informed consent to participate in the experiment. The study was approved by the Korean Advanced Institute of Science and Technology Institutional Review Boards in accordance with the Declaration of Helsinki.

Standardization of emotional stimuli

Stimuli consisted of forty-five emotional faces and forty-five text-based emotional emoticons. Forty-five faces expressing happy, sad, and neutral emotions were selected from the Korean Facial Expressions of Emoticon (KOFEE) database (J. Y. Park et al., 2011). Text-based happy and sad emoticons were searched for on the world-wide web. Then we produced scrambled emoticons that did not have configurable information, and then these scrambled emoticons were used as emoticons of a neutral condition. Ninety emotional expressions, including faces and text-based emoticons, were standardized in independent samples consisting of forty-seven healthy volunteers (21 females, mean age of 28.43 ± 4.31 years). These participants were asked to rate the feeling they have felt toward emotional expressions composed of 90 stimuli (45 faces and 45 facial emoticons of happy, neutral, and sad emotions) on an 11 point Likert scale (-5 to +5). We compared the mean absolute value of four emotional expressions that we called 'feeling intensity' or 'emotionality' (Citron, Gray, Critchley, Weekes, & Ferstl, 2014). Repeated measures analysis of variance (RANOVA) of 2 (face, emoticon) by 3 valences (happy, sad, neutral) design were performed on the emotionality score. There was a significant main effect of valence ($F(1.744, 80.228) = 272.618$, $P < 0.001$, Greenhouse-Geisser corrected), while there were no differences between emoticons and faces ($F(1, 46) = 0.011$, $P = 0.919$) and no interaction between those two main effects ($F(1.685, 77.488) = 0.285$, $P = 0.818$, Greenhouse-Geisser corrected). In addition, a post-hoc t-test revealed that there was no difference between sad and happy conditions ($P = 0.082$) with a significant difference between emotional and neutral conditions ($P < 0.001$ in both sad and happy contrast to neutral). Additionally, participants of the main experiments also underwent the rating procedure above before the MEG recording.

MEG experimental task

During the MEG recording, ninety stimuli consisting of 45 faces and 45 text-based emoticons were presented in the center of the screen using in-house software, the KRISSMEG Stimulator 4. The size, duration, and stimulus onset asynchrony (SOA) of all the stimuli were 27×18 cm, 500ms and 1500ms, respectively, and the order of stimuli presentation was pseudo-randomized. Participants completed 4 runs and each run contained 180 stimuli (30 sad faces, 30 happy faces, 30 neutral faces, 30 sad emoticons, 30 happy emoticons, 30 neutral emoticons each) and took 270s. In addition, to maintain the participants' attention to task, the participants were instructed to discriminate between sad and happy by pressing a button when a question mark appeared. The question mark randomly appeared on the screen every 9 to 15 trials.

Acquisition

A 152-channel MEG system (KRISS MEG, Daejeon, Korea, 152 axial first-order double-relaxation oscillation superconducting quantum interference device (DROS) gradiometers) covering the whole head was used to make MEG recordings in a magnetically shielded room for 60–90 minutes at a sampling rate of 1,024 Hz. The relative positions of the head and the MEG sensors were determined by attaching four small positioning coils to the head. The positions of the coils were recorded at intervals of 10–15 min by the MEG sensors to allow co-registration with individual anatomical MRI data. The maximum difference between head positions before and after the run was deviation < 2mm and goodness of fit (GoF) > 95%. The EEG system for eye and muscle artifacts recordings were made simultaneously with the MEG recordings. During MEG recording, participants were seated with their heads leaning backward in the MEG helmet. The translation between the MEG coordinate systems and each participant's structural MRI was made using four head position coils placed on the scalp and fiducial landmarks (Hämäläinen, Hari, Ilmoniemi, Knuutila, & Lounasmaa, 1993).

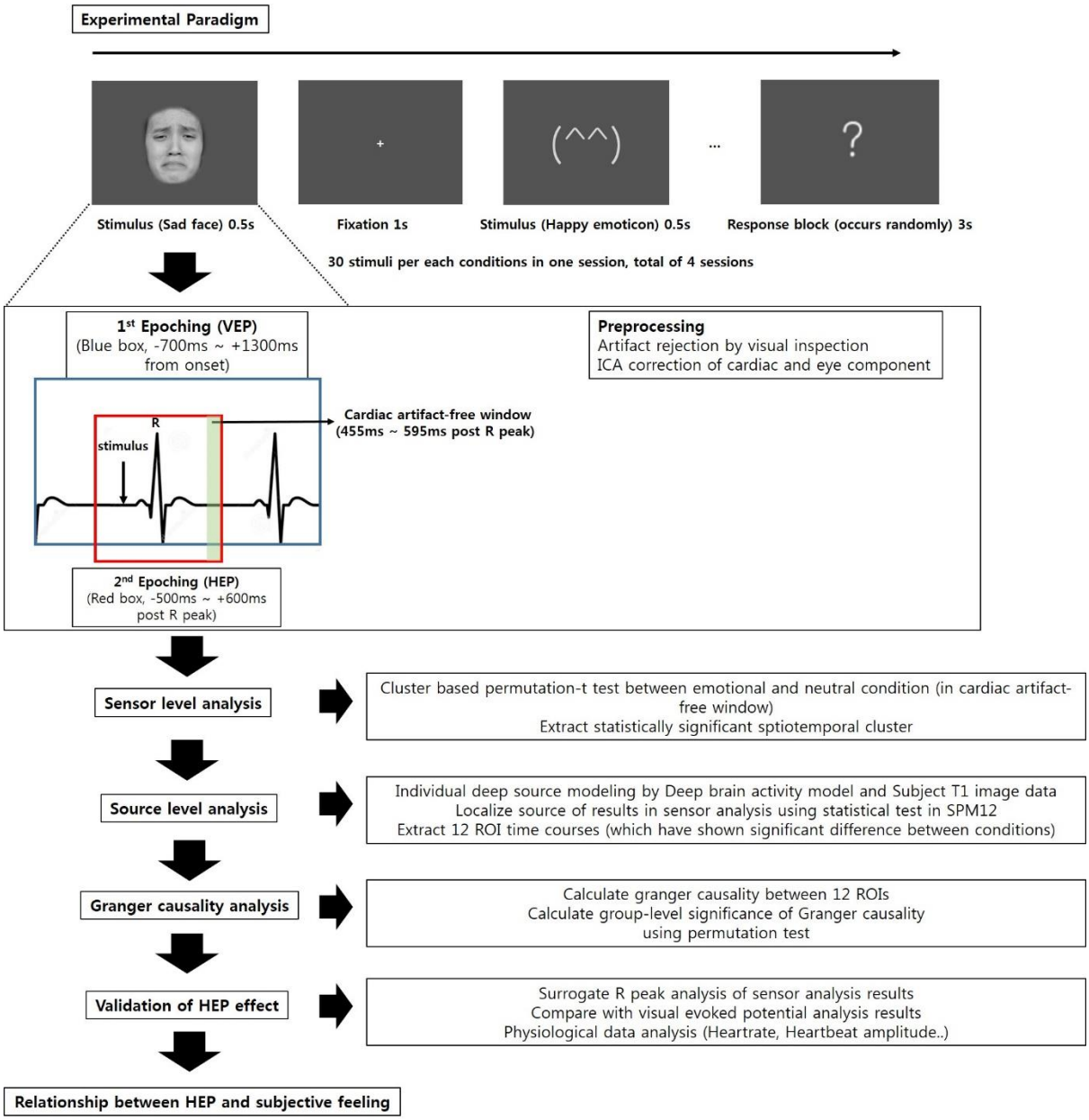

Figure 1. Overall experimental flow

Data preprocessing

Data were processed with a Fieldtrip toolbox (Oostenveld, Fries, Maris, & Schoffelen, 2011). First, raw data were epoched from 700ms before stimulus onset to 1300ms after stimulus onset. Epochs containing large artifacts were rejected by visual inspection. After artifact trial rejection,

the eye movement artifact and the cardiac field artifact were removed by independent component analysis (ICA) using the function "ft_componentanalysis" with the runICA algorithm. Twenty components were identified for each six conditions. Two neurologists visually inspected each component, and components that showed typical spatial and temporal patterns of the cardiac field artifact, eye blinking and movement noise were removed. After removing the noise, the data were filtered with a 1-40 Hz Butterworth filter. Then, the heartbeat evoked potential (HEP) for each stimulus condition was extracted by subsequent epoching which was time-locked to the R peak of every epoch. R peaks were detected using the Pan-Tompkins algorithm (Pan & Tompkins, 1985) and the HEP of each condition was extracted by epoching 500 ms before the R peak to 600 ms after the R peak in the epoch of each condition. Because a heartbeat enters the central nervous system (CNS) around 200ms after the R peak by vagal afferent stimulation at the carotid body (Eckberg & Sleight, 1992) and a visual stimulus enters the CNS immediately through the retina, a heartbeat that occurs before a -200ms visual stimulus onset stimulates the brain earlier than a visual stimulus onset. Therefore, we excluded R peaks that occurred before 200 ms of a stimulus onset to include heartbeat evoked processing that occurred only after visual stimulus. Therefore, this procedure excluded cortical input of a heartbeat that has occurred before the visual stimulus. The R peak after 700ms of stimulus onset was also excluded because that HEP epoch would contain the next visual stimulus onset. Finally, a baseline correction was performed using a pre-R-peak interval of 300ms and trials of the same condition for each subject were averaged.

Sensor analysis

Cluster-based permutation based paired t-test between each emotional condition and neutral condition

We compared the HEP of the emotional condition and a neutral condition. Four tests were performed including a sad face vs. a neutral face, a happy face vs. a neutral face, a sad emoticon vs. a neutral emoticon, a happy emoticon vs. a neutral emoticon. To deal with multiple comparison problems, we used a cluster-based permutation paired t test. These tests were done as follows. First, paired t tests were performed at all time points between 455 and 595 ms and all sensors. Then significant spatiotemporal points of uncorrected p-values below 0.05 (two-tailed) were clustered by the spatiotemporal distance and the summed t-value of each cluster were calculated. After calculating the cluster t-stat, permutation distribution was made by switching condition labels within subjects randomly, calculating the t-value, forming clusters as mentioned above, selecting the maximum cluster t-value and repeating this procedure 5000 times. Finally, after the maximum cluster t-values of each permutation made the permutation distribution, the corrected p-value original clusters were calculated. A time window of 455-595ms after each R peak, which is known to have the minimal influence on the cardiac field effect (less than 1%) was submitted as input of the test. Data were downsampled to 128 Hz to make the computation efficient.

Source analysis

Source reconstruction was implemented in the MATLAB package Brainstorm (Tadel, Baillet, Mosher, Pantazis, & Leahy, 2011). To estimate the time courses of both cortical and subcortical activity, we used the default settings in open source Matlab toolbox Brainstorm's implementation of the Deep Brain Activity model using the minimum norm estimate (MNE) (Attal & Schwartz, 2013; Tadel et al., 2011). First, cortical surfaces and subcortical structures, including the amygdala and basal ganglia, were generated for each subject from 3T MPRAGE T1 images using Freesurfer (Fischl, 2012). The individual heads/parcellations were then read

into Brainstorm (Tadel et al., 2011) along with track head points to refine the MRI registration. In Brainstorm, a mixed surface/volume model was generated, and 15,000 dipoles were generated on the cortical surface and another 15,000 dipoles were generated in subcortical structure volume. Refining the registration with the head points improves the initial MRI/MEG registration by fitting the head points digitized at the MEG acquisition and the scalp surface. Using the individual T1 images and transformation matrix generated as above, a forward model was computed for each subject using a realistic overlapping spheres model. The source activity for each subject was computed using the MNE (Brainstorm default parameters were used). The source map was averaged over a time window of 488ms to 515ms - which showed a significant difference between a sad face and a neutral face at a sensor level (other emotional conditions were not significantly different from neutral conditions). Then this averaged spatial map was exported to SPM12 software (Wellcome Department of Cognitive Neurology, London, UK, http://www.fil.ion.ucl.ac.uk/spm) and subsequent statistical tests were performed. Paired-t tests were used to identify regions that had a different HEP time course within the selected time window between the sad face and the neutral face. Moreover, to test the absolute activation difference between two conditions, we additionally exported the absolute spatial map to SPM12 and applied the paired t-test design.

Granger causality analysis of HEP source activity

After identifying brain regions that had different time courses, we performed a Granger causality analysis (Barnett & Seth, 2014) on time courses of those regions to determine whether effective connectivity between those regions is modulated differently in emotional expression condition compared to the neutral condition. In Granger causality (Granger, 1988) analysis, it says that time course Y G causes time course X if the past time points of Y and X explains X

better than the past of X alone. It is formulated by the log-likelihood ratio between the residual covariance matrix of the model that explains X by the past of X and Y and the residual covariance matrix of the model that explains X by the past of X alone (Barnett & Seth, 2014).

$$\boldsymbol{X}_t = \sum_{k=1}^{p} A_{xx,k} \cdot \boldsymbol{X}_{t-k} + \sum_{k=1}^{p} A_{xy,k} \cdot \boldsymbol{Y}_{t-k} + \boldsymbol{\varepsilon}_{x,t}$$

$$\boldsymbol{X}_t = \sum_{k=1}^{p} A'_{xx,k} \cdot \boldsymbol{X}_{t-k} + \boldsymbol{\varepsilon}'_{x,t}$$

$$F_{\boldsymbol{Y}\rightarrow\boldsymbol{X}} = \ln |\Sigma'_{xx}|/|\Sigma_{xx}|$$

where A is the matrix of the regression coefficient, Epsilon is the residual, Sigma is the covariance matrix of the residual, and F is the Granger causality of X and Y. All these calculations were done using a multivariate Granger causality toolbox (MVGC toolbox) (Barnett & Seth, 2014).

To calculate the Granger causality, we first extracted the absolute source time courses (455ms-595ms after the R peak) of twelve regions of interest (ROI), which showed the difference between conditions in our previous source analysis for every trial for each subject. This process resulted in three-dimensional matrices of 12 (ROI) * a number of time points in each trial * the number of trials for every subject and were used as input for the Granger causality analysis. ROIs include the right anterior insula (RAI), right posterior insula (RPI), bilateral anterior cingulate cortex (RACC and LACC), right globus pallidus (RGP), right putamen (RP), right amygdala (RAMG), right superior prefrontal cortex (RSFG), right middle prefrontal cortex (RMFG), right inferior frontal cortex (RIFG), right ventromedial prefrontal cortex (RvmPFC), and left orbitofrontal cortex (LOFC). The subcortical structure, the RGP, RP, and RAMG, was chosen as single volume while other cortical ROIs were defined by a single voxel that was significant in the source analysis and surrounding voxels. Detailed information of the ROIs,

including the coordinates, size and inclusion criteria, are provided in the supplementary materials. (Briefly, regions that have shown a significant difference below a cluster level FDR corrected threshold of $p < 0.05$ in the paired test between two conditions were used as ROIs.) After extracting the time courses of 12 ROIs, we preformed a Granger causality analysis on that ROI time courses of each subject using the MVGC toolbox (Seth et al, 2014). This analysis returned a 12 by 12 Granger causality matrix which consisted of the Granger causality of each pair of ROIs for every subject. To test the group-level significance of the averaged Granger causality over a subject, we used a permutation method. We generated 1000 surrogate Granger causality matrices to make the permutation distribution of the averaged Granger causality. For each iteration, we permuted half of the trials between the emotional condition and neutral condition for each subject. Then, the Granger causality matrix of every subject was computed and these matrices were averaged over subjects. These processes were iterated for 1000 times so that 1000 surrogate averaged Granger causality matrices were generated. Finally, the statistical significance of the original Granger causality matrix was tested by finding the position of original Granger causality in permutation distribution. These surrogate Granger causality matrix analyses were done for an emotional condition, neutral condition, and emotional – neutral condition separately. In addition, because Granger causality is positively biased (Barnett, Seth, 2014), the significance value was calculated in a one-tailed fashion to determine whether or not the Granger causality in emotional and neutral condition is significantly larger. In contrast, in the emotional-neutral condition, the significance value was calculated in a two-tailed method because it has a symmetric distribution reflecting both increased and decreased Granger causality. In addition, to use a sufficient number of time points in the Granger causality analysis, we used data that were resampled to 512 Hz (the previous sensor and source analysis used 128 Hz data).

Analysis of physiological data

Heartbeat distribution in each condition

To show that the HEP effect does not result from a biased heartbeat distribution, within the original visual epoch, we divided the visual epoch between -200ms and 700ms, which was the beginning and end of the HEP epoching, by 100ms time windows (total of nine time bins) and counted how many heartbeats there were in those time windows. We did this for every condition. Then, the analysis of variance between nine time bins was performed to test whether the occurrence of heartbeats was the same in every time bin.

Heartrate modulation in each condition

The heartrate in every condition was calculated for each subject. Then, an analysis of variance between every condition was performed to test whether the heartrate were different across conditions.

Analysis to exclude effect of visual processing

Surrogate R peak analysis

To test whether the HEP modulation effect is time-locked to the heartbeat, we created 100 surrogate heartbeats that were independent of original heartbeats (H.-D. Park et al., 2016; H.-D. Park et al., 2014). Then we computed the surrogate HEP with surrogate heartbeats and performed the same cluster based permutation t-test between conditions that showed a significant difference in the sensor level analysis. Finally, we made the distribution of maximum cluster statistics of a surrogate R peak and the calculated position of our original cluster statistics in this distribution to show that the heartbeat-locked effect is significantly large

in such a distribution.

Analysis of visual evoked potential (VEP)

To test whether or not the HEP modulation effect is confounded by the visual evoked potential effect, we performed the same cluster based permutation test with a visual stimulus-locked potential and compared the topology of significant clusters between HEP clusters and VEP the sensor level. Then, we performed the source localization of the VEP activity in a significant cluster time window and exported it to SPM12 to perform a statistical test between emotional and neutral conditions with the same methods used in the HEP analysis (including the absolute value difference). Then we compared resulting source with the result of the HEP analysis. This VEP analysis was not done for all conditions but for conditions that had a significant HEP modulation effect so that we could compare significant modulation of the HEP with the VEP effect. (In our experiment, the sad face was the only condition that had a significant HEP modulation.)

Results

Sensor analysis

Significant difference in the HEP between sad face and neutral face perception

A HEP cluster showing a significant difference between sad face and neutral face perception was found in the right frontocentral sensors within a 488ms-515ms time range (Monte-Carlo p = 0.046). In other conditions, including happy face vs neutral face (Monte-Carlo p = 0.396), sad emoticon vs neutral emoticon (Monte-Carlo p = 0.857), happy emoticon vs neutral emoticon (Monte-Carlo p = 0.710), there were no significantly different clusters showing a different HEP amplitude.

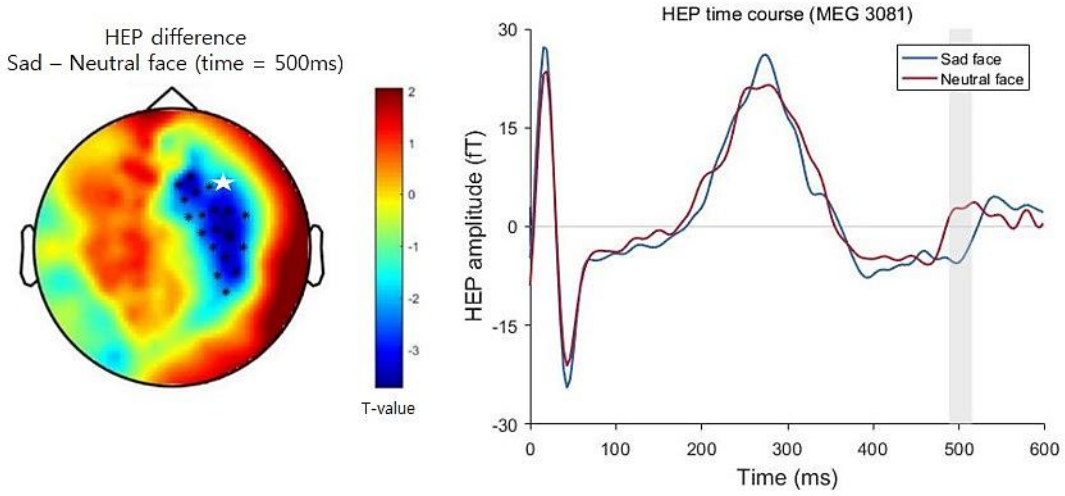

Figure 2. Topographic map (left) of the differences in HEP between sad vs. neutral face conditions and a single channel plot among significant clusters (right) – The channel plotted in the right figure are marked as a white star in the left topographic map.

Figure 2 (left) – source data 1

Statistical result of differences in HEP between sad vs. neutral face (in cluster based permutation t test).

Figure 2 (right) – source data 2

Time course of HEP (fT) induced by sad vs. neutral face in 455ms ~ 595ms time window in MEG3081 sensor.

Source analysis

Interoceptive network and prefrontal-basal ganglia network as sources of HEP modulation in sad faces

To find the brain region underlying modulation of the HEP in sad face conditions, source reconstructions of the MEG signal in a sad face and neutral face were done in brainstorm and

paired t-test of the two conditions were done in SPM12 (with a spatial map that was averaged within the time range of 488ms-515ms after the R peak). With the cluster-forming threshold using p-value = 0.01 and 10 adjacent voxels, several regions that have different HEP time courses between a sad face and a neutral face were identified. Four significant clusters appeared. Briefly, these clusters included the right prefrontal cortices, anterior insula, anterior cingulate cortex, and basal ganglia. More specifically, the first cluster (red, p = 0.003, cluster level family-wise error (FWE) corrected) included the right prefrontal regions that consisted of the right superior frontal gyrus (RSFG), which is close to the dorsomedial prefrontal cortex (dmPFC), and the middle frontal gyrus (RMFG), which corresponded to the dorsolateral prefrontal cortex (dlPFC). The second cluster (green, p = 0.001, cluster level FWE corrected) included the right anterior insula (RAI) and the right putamen (RP). The third cluster (blue, p = 0.003, cluster level FWE corrected) included the right anterior cingulate cortex (RACC) and the left anterior cingulate cortex (LACC). Finally, the fourth cluster (pink, p < 0.001, cluster level FWE corrected) included the right basal ganglia, which consisted of the right globus pallidus (RGP) and right putamen (RP). Previous studies reported ACC and AI as a source of HEP (Couto et al., 2015; H.-D. Park et al., 2017; H.-D. Park et al., 2014). Additionally, in a paired t-test using the absolute value of time courses, right ventromedial prefrontal cortex (RvmPFC) and left orbitofrontal cortex (LOFC) clusters were found, which is also a region known to process interoceptive information; a detailed result of this analysis is provided in the supplementary materials.

Table 1. Clusters showing significant different time courses between sad face and neutral face conditions

Cluster	Region	MNI coordinate	Cluster size (voxel number)	F value	Cluster P value (FWE corrected)
Cluster 1 (Red)	Rt. SFG	21 20 42	311	23.13	0.003
	Rt. MFG	33 18 36		12.86	
Cluster 2 (Green)	Rt. AI	27 24 6	379	20.02	0.001
	Rt. Putamen	31 6 8		12.08	
Cluster 3 (Blue)	Rt. ACC	9 40 10	313	17.32	0.003
	Lt. ACC	-3 22 28		14.68	
Cluster 4 (Pink)	Rt. putamen	27 -8 0	412	16.59	<0.001
	Rt. GP	21 0 2		15.30	

SFG: superior frontal gyrus, AI: anterior insula, MFG: middle frontal gyrus, ACC: anterior cingulate cortex, GP: globus pallidus (voxel size: 1mm x 1mm x 1mm)

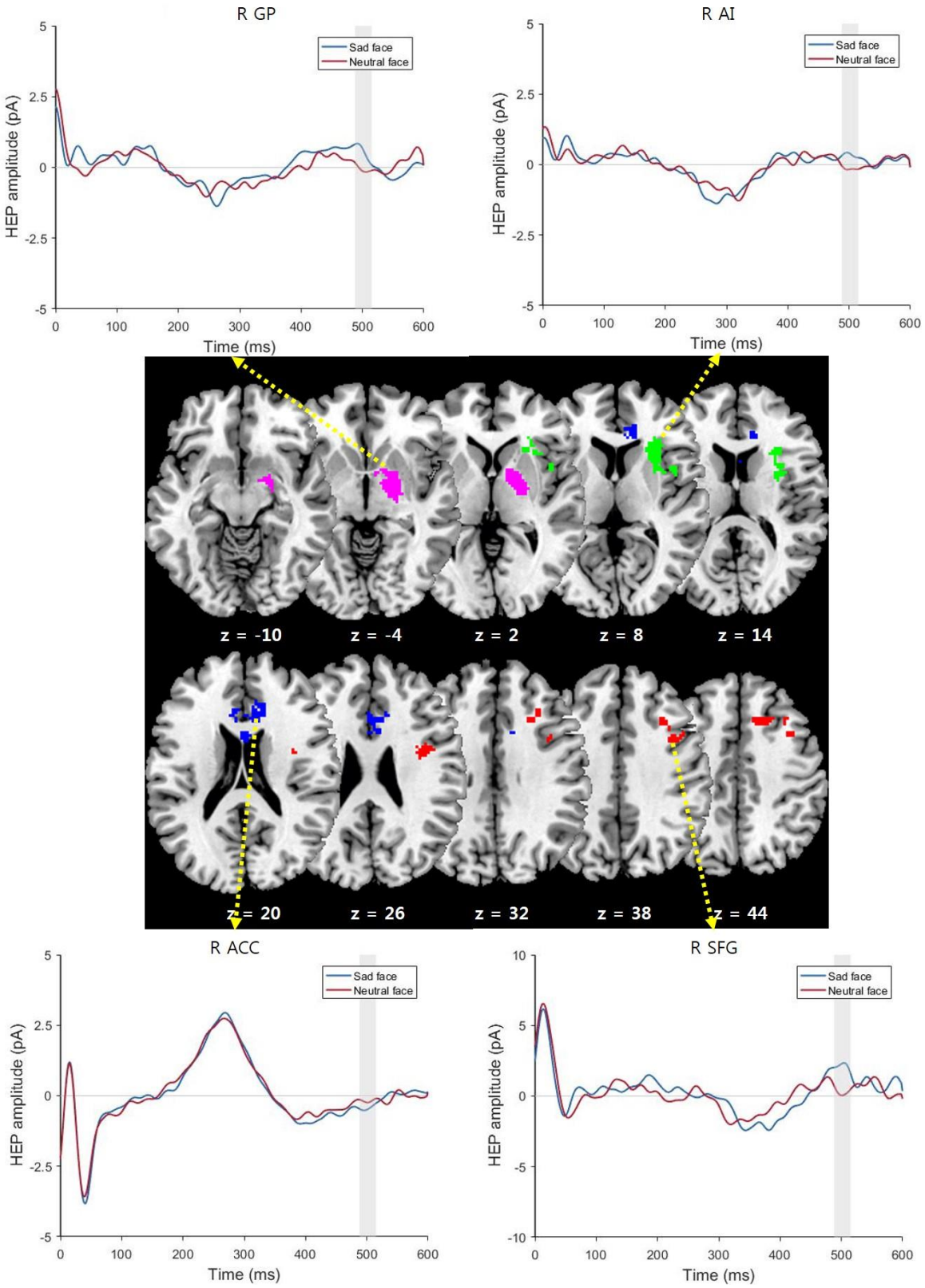

Figure 3. Brain regions showing differencies in HEP modulation in the contrast of sad vs. neutral face conditions and the mean time courses of HEP from 25 voxels around peak

voxels (the yellow dashed arrow connects the region of cluster and corresponding time courses of that region)

Granger causalities among brain regions

Increased bottom up interoceptive information from the right posterior insula to the right anterior insula to the right anterior cingulate cortex in sad face perception.

To investigate the causal relationship among regions that have shown differential HEP time courses between the sad face and neutral face, we performed a Granger causality analysis within these regions. Selection criteria of ROIs are provided in supplementary materials. In the Granger causality analysis results, the Granger causality from RPI to RAI (Monte-Carlo $p = 0.04$) and RAI to RACC increased (Monte-Carlo $p = 0.032$) in sad face HEP processing over that of the neutral face, which reflects increased bottom-up interoceptive information processing (Craig & Craig, 2009; Simmons et al., 2013; Smith & Lane, 2015). Moreover, the Granger causality from GP to both RSFG and RMFG increased (Monte-Carlo $p = 0.018$ and 0.014 each) which reflects an increase in pallidoprefrontal information flow. However, the Granger causality from RACC to RMFG (Monte-Carlo $p = 0.024$) and LOFC to RvmPFC (Monte-Carlo $p = 0.04$) decreased. Except for these modulations in the sad face, significant Granger causality matrix patterns in the sad face and neutral face were similar. Detailed information of all statistical results is provided in the supplementary materials.

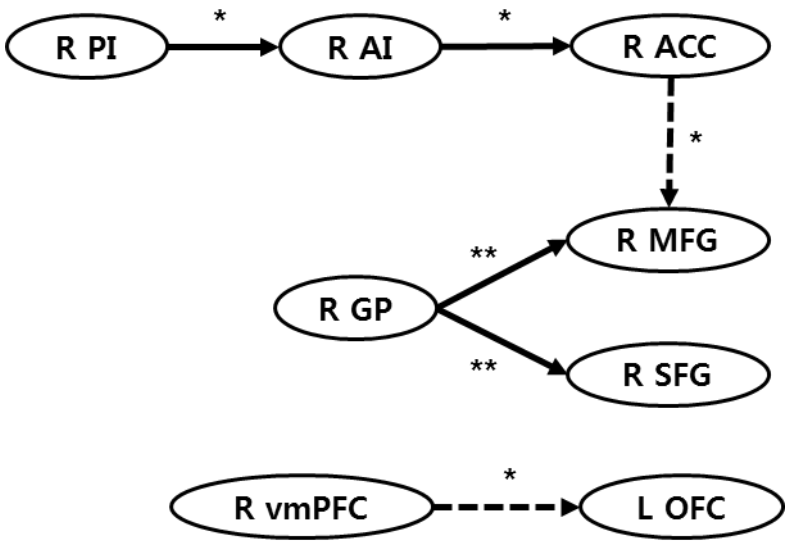

Figure 4. Enhanced bottom up interoceptive information processing in sad face perception (solid arrow: significantly enhanced Granger causality in sad face > neutral face, dashed arrow: significantly decreased Granger causality, * p < 0.05, ** p < 0.01; the value of the Granger causality above is the difference between the averaged Granger causality of each condition)

Analysis of physiological data

Heart rate and ECG R peak amplitude modulation in each condition

To determine whether the effect of the different HEP amplitude originated from different heart-related physiological statuses, the heart rate and ECG R peak amplitude were compared between the conditions using one-way RANOVA. There were no significant differences between conditions in either heart rate ($F(1.516, 46.982) = 2.367$, $p = 0.118$, Greenhouse-Geisser corrected) or heartbeat amplitude ($F(2.989, 92.658) = 0.958$, $p = 0.416$, Greenhouse-Geisser corrected).

Heartbeat distribution in each condition

To rule out the possibility that our significant HEP modulation effect resulted from the fact that the heartbeat appeared more or less in a specific time window of visual evoked cortical processing, distribution of heartbeat occurrences within each time window of visual processing was analyzed. Two-way 6*9 RANOVA (six condition and nine 100ms time bins (-200ms from 700ms to visual stimulus onset)) showed neither a different occurrence rate of heartbeat among the conditions (F (3.810, 118.111) = 0.783, p = 0. 533, Greenhouse-Geisser corrected) nor among time bins (F (4.876, 151.143) = 1.540, p = 0.182, Greenhouse-Geisser corrected).

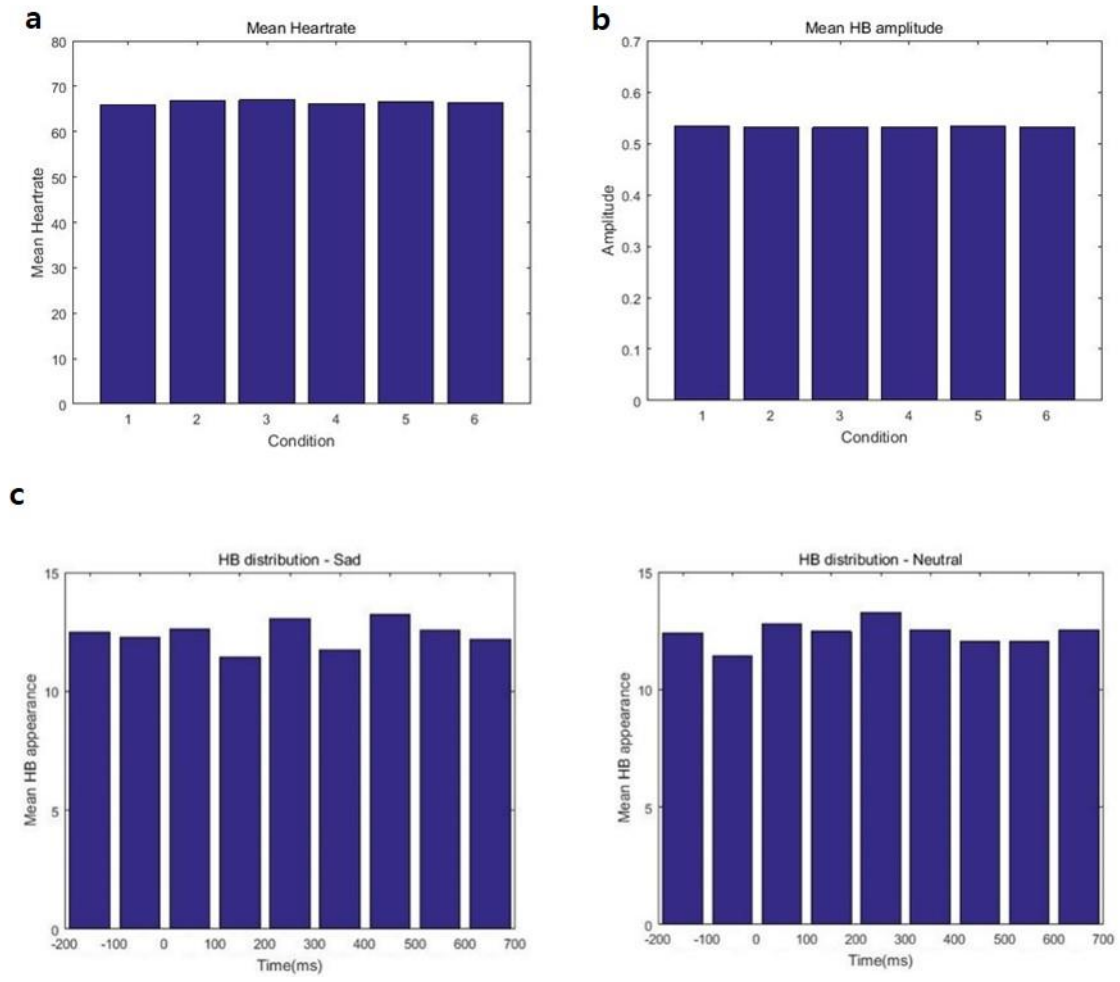

Figure 5. Physiological data analysis results - a. mean heartrate of six experimental conditions b. mean R peak amplitude of six experimental conditions, c. mean R peak occurrence distribution in epoch of sad face (left) and neutral face (right)

Analysis to exclude the effect of visual processing

Surrogate R peak analysis on HEP modulation effect of a sad face

One hundred surrogate R peaks were made to make random epochs that were independent of a heartbeat. Then, the maximum summed cluster t statistics of the difference between sad and neutral faces was calculated and used to make a permutation distribution. Our HEP modulation effect size (maximum cluster t statistics) was significant in that the distribution (Monte-Carlo $p<0.03$) meant that our effect was highly likely to be locked to the heartbeat.

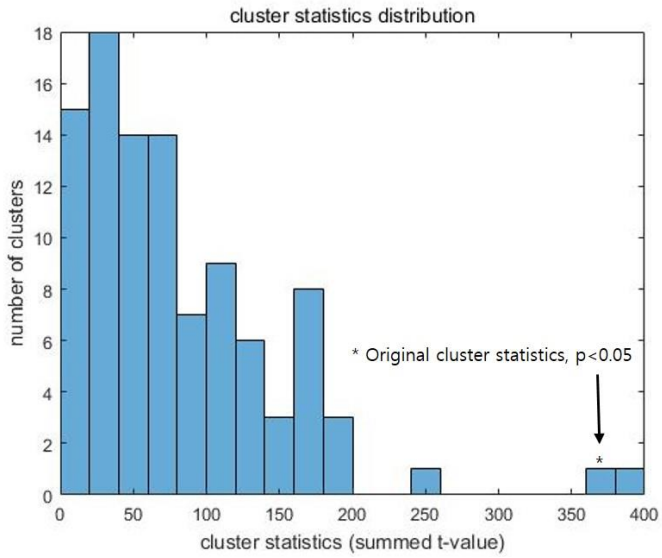

Figure 6. The surrogate R peak histogram (absolute cluster statistics), * represents the location of the original cluster statistic of the HEP modulation effect in a sad face

Different spatial pattern between visual evoked potential analysis (VEP) results and HEP analysis results in sad face perception

Finally, to exclude the possibility that HEP modulation was confounded by neural activity reflecting visual processing, we analyzed visualevoked potential data with a cluster based

permutation t-test. Two significant clusters at 73ms-198ms (Monte-Carlo $p = 0.05$) and 815ms-948ms (Monte-Carlo $p = 0.004$) after stimulus were found. However, their topological distribution was totally different from the HEP effect. Furthermore, in the source analysis of VEP (which was performed with the same method as the HEP source analysis), two clusters, which included the right ventromedial prefrontal cortex cluster and right cuneus cluster, were found at 73ms-198ms (cluster-forming threshold = 0.01, minimum number of adjacent significant voxels = 10, cluster level p-value < 0.001 in both clusters). Two clusters were also found in the 815ms-948ms time window, which included the left cuneus cluster and the right cuneus cluster ($p < 0.001$, $p = 0.042$ each with the same cluster definition of the earlier cluster). Finally, in the paired t-test of absolute time courses, the right fusiform/middle temporal gyrus cluster (cluster level $p < 0.001$) and the right angular gyrus/superior temporal gyrus cluster (cluster level $p = 0.043$, FWE corrected) were more activated in the sad face of the 73ms-198ms window, while a supplementary motor area cluster (cluster level p-value = 0.003, FWE corrected) was found in the late time window (815ms-948ms). Detailed information on the absolute time courses, including statistical information, is provided in the supplementary materials.

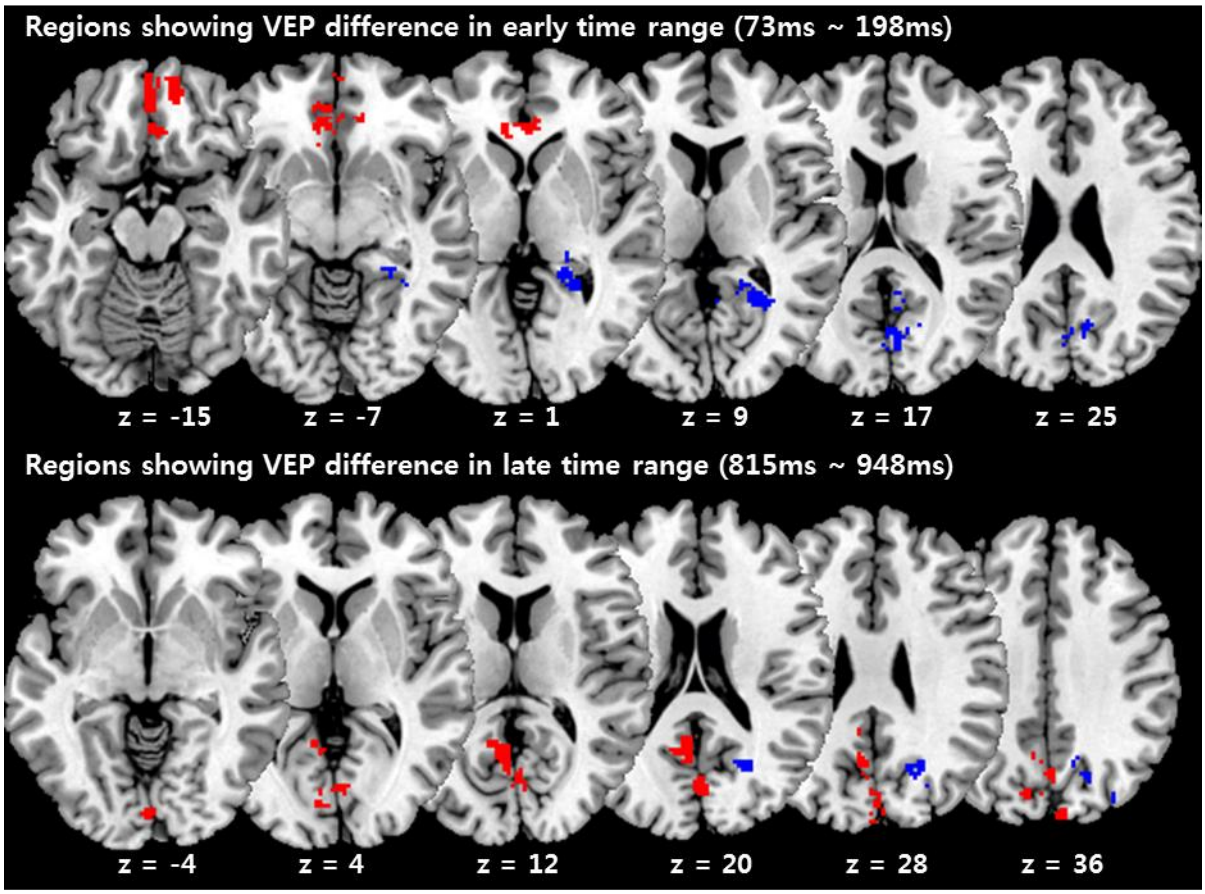

Figure 7. Regions showing significantly different VEP for a sad face compared to a neutral face (upper: 73ms-198ms, lower: 815ms-948ms)

Table 2. Regions showing significantly different VEP for a sad face compared to a neutral face (73ms-198ms, 815ms-948ms)

Cluster (73ms-198ms)	Region	MNI coordinate	Cluster size (voxel number)	F value	Cluster P value (FWE corrected)
Cluster 1 (Red)	Rt superior orbital gyrus	11 56 -17	576	18.18	<0.001
	Rt medial orbital gyrus	11 36 -10		15.59	
	Lt gyrus rectus	-1 50 -15		14.65	
Cluster 2 (Blue) Rt Cuneus	Rt cuneus	3 -73 18	465	18.17	<0.001
	Rt cuneus	11 -68 26		14.48	
	Rt calcarine sulcus	23 -48 6		14.18	
Cluster (815ms-948ms)	**Region**	**MNI coordinate**	**Cluster size (voxel number)**	**F value**	**Cluster P value (FWE corrected)**
Cluster 1 (Red)	Lt calcarine sulcus	-3 -62 14	836	33.02	<0.001
	Lt cuneus	-1 -73 20		25.06	
	Lt calcarine sulcus	-1 -87 -4		23.78	
Cluster 2 (Blue) Rt Cuneus	Rt cuneus	23 -68 24	199	20.46	0.042
	Rt superior occipital gyrus	28 -78 34		15.89	
	Rt superior occipital gyrus	23 -73 30		12.15	

(voxel size: 1mm x 1mm x 1mm)

Discussion

Our findings provide direct and strong evidence that perception of a sad face modulates the interoceptive information processing in the cortex.

First, we showed that cortical heartbeat processing after presentation of a sad face has significantly different spatiotemporal dynamics compared with a neutral face and these differences are localized in the interoceptive network (AI, ACC, vmPFC), basal ganglia (GP, Putamen) and prefrontal areas (MFG, SFG).Importantly, results of the Granger causality analysis of these regions showed that bottom up heartbeat information processing from RPI to RAI to RACC were increased. In contrast to the HEP results, visual – locked activity was different in the bilateral visual information processing area including the bilateral cuneus, fusiform face area and other areas including the ventromedial prefrontal cortex and supplementary motor area. Interestingly, the only region that overlapped between the HEP and VEP were vmPFC – which is a key region in somatic marker hypothesis. Finally, surrogate R peak analysis provided strong evidence that our result is a consequence of cortical heartbeat processing modulation. Additionally, analysis of physiological data and cardiac artifact removal using ICA also ruled out the possibility of an effect of other physiological effects on the cortical signal.

Our results go beyond previous studies of interoception and emotion in several aspects.

The result of our sensor analysis showed that a sad face evoked a different spatiotemporal pattern of HEP in the right frontal and central sensors at a time window centered about 500ms after the R peak, which was different from the pattern for a neutral face. Two recent studies with electroencephalography (EEG) have reported the HEP modulation by emotional stimuli. One study using visual and auditory stimuli showed the HEP modulation by high-arousal mood

induction in left parietal clusters at 305 to 360ms after the R peak and the right temporoparietal cluster at 380 to 460ms after the R peak (Luft & Bhattacharya, 2015). They summed both positive and negative emotional valence conditions to show arousal effect. The other recent EEG study in 5 month old infants reported that a video clip of an angry or fearful face increases HEP at 150 to 300ms after R peak in the frontal cluster (Maister, Tang, & Tsakiris, 2017). While both happy and sad stimuli are low-arousal emotions (Liu, Chen, Hsieh, & Chen, 2015), the second study neither showed the significant cluster in the contrast of happiness vs. neutral conditions nor applied sad stimuli. Thus, the HEP modulation by emotional stimuli reported in two recent studies reflect the effect by emotional arousal more likely than conceptualizing process. In addition, both studies did not demonstrate underlying neural mechanism of this modulation effect based on source analysis. Considering that the bodily signal not only need to be recognized in brain but also need to be conceptualized to make emotional feeling (Smith & Lane, 2015), we insist that our result reflects the conceptualization process of interoceptive signals that are related to specific emotional feelings, but not just arousal which is related to early representation of bodily signal. First, a sad face used in this study is known to induce a relatively low arousal (Liu et al., 2015). Second, the spatiotemporal dynamics of our results are clearly different from the emotional arousal effect of Luft et al and Maister et al. In their study, HEP differences were shown in the parietal and temporal clusters before 460ms post R peak (Luft & Bhattacharya, 2015) and 150 to 300ms after R peak in the frontal ROI (Maister et al., 2017), whereas our results were found at the frontal and central sensors around 500ms post R peak (which is later than in the arousal effect). Third, anterior cingulate cortex is thought to be related to forming emotion concept based on whole body representation of insula (Smith & Lane, 2015) which is consistent with our results that have shown increased Granger causality from the insula to anterior cingulate cortex. Considering these aspects, our results are not likely to be caused only by emotional arousal and are likely to be related to later processing, which

we suggest is related to conceptualization and making of individual emotional feeling. Additionally, the topology of our result is similar to Shao et al. which showed that HEP suppression in the right frontal and central sensors is induced by pain (Shao et al, 2011, clinical neurophysiology). Contrary to a sad face, other emotional expressions, including a sad emoticon, happy face and happy emoticon, did not show a significant HEP modulation effect. In particular, a sad emoticon, which is also a sad emotional expression like a sad face, did not modulate HEP although the emotionality scores of a sad face and a sad emoticon were not different (in paired-t test, $p = 0.492$, mean emotionality score of sad emoticon = 2.81, mean emotionality score of sad face = 2.71). Considering that a text based emoticon is not an innately encoded stimulus like a face, responses to sad emoticons are more likely to be influenced by experiences with sad emoticons or emotional experience associated with sad emoticons, which are different from sad faces. Therefore, we suspected that a sad emoticon would have induced a more variable intensity of feeling across subjects and thus a more variable size of the HEP modulation effect, which might have caused a statistically insignificant modulation effect, while some people who are susceptible to sad emoticons might have exhibited HEP modulation effect by a sad emoticon. In accordance with this explanation, our participants showed a more heterogeneous response toward sad emoticons than toward sad faces. Variance of mean emotionality score in the sad emoticon across subjects was 0.85, which is much larger than the variance of the sad face (0.31).

In source analysis of HEP and VEP modulation by s sad face, we found that there are two clearly distinct systems of processing, cardiac information processing and visual information processing. First, brain regions that reflect HEP modulation in sensor analysis were found in RAI and RACC, which is a previously known source of HEP (Couto et al., 2015; H.-D. Park et al., 2017; H.-D. Park et al., 2014; Pollatos, Kirsch, & Schandry, 2005). These regions are

also identified as an overlapping region of emotion, interoception and social cognition in a recent meta-analysis (Adolfi et al., 2016). Moreover, a Granger causality analysis revealed that cardiac information flow from RPI to RAI to RACC increases with sad face perception. Interoceptive sensory information is primarily represented in the posterior insula (Barrett & Simmons, 2015; Craig & Craig, 2009) and this interoceptive information is relayed and integrated into the anterior insula to form conscious emotional concept – feeling (A. Damasio & Carvalho, 2013; Smith & Lane, 2015). Moreover, the anterior insula interacts with many regions, including the ACC, which is a central autonomic network (CAN) that regulates autonomic function (Beissner, Meissner, Bär, & Napadow, 2013). These previous studies make it clear that bottom-up cardiac information flow is increased in sad face perception. However, according to the the source analysis of VEP, only the visual cortical region and ventromedial prefrontal regions appeared, which is consistent with previous EEG/MEG studies of sad faces (Batty & Taylor, 2003; Esslen, Pascual-Marqui, Hell, Kochi, & Lehmann, 2004). By integrating these results, we firmly insist that processing of sad faces involves distinct interoceptive processing and visual processing and this is revealed by the HEP and VEP after the stimulus. To our knowledge, this is the first study that has shown distinctive processing of both systems of processing induced for sad faces in a clear and direct way. These results well correspond to hypotheses that explain the relationship between emotion and interoception like the somatic marker hypothesis (A. R. Damasio, 2003), which predicts that bottom up interoceptive processing would be increased by emotional stimulus. The somatic marker hypothesis predicts that physiological change would be induced by emotional stimulus and modulates brain-body interaction while the result of our physiological data analysis showed that cardiac activity parameters, including heartrate and heartbeat amplitude, were not modulated in the sad face. However, considering that direct input of the HEP is pressure in the carotid baroreceptor and that we did not measure blood pressure or index of carotid stimulation, it is hard to tell whether

there was no physiological change. Another possibility is that absence of induced physiological change might be due to our short stimulus onset asynchrony of about 1 second, in which it is hard to evaluate physiological changes like heart rate modulation, which occurs after several seconds (Critchley et al., 2005). Note that, our results derived from sad emotion among negative ones. Therefore, future experiments are needed to be performed with other negative emotional stimuli such as fear or anger.

What is the unexpected and surprising result is that cardiac information processing in the basal ganglia (RGP/RP) and prefrontal regions (SFG/MFG) is also modulated. Moreover, Granger causality analysis revealed that information flow from GP to SFG/MFG is increased. Globus pallidus is known to send input to the prefrontal cortex via the thalamus. This pathway is related to initiating motor action (Singh-Bains, Waldvogel, & Faull, 2016). In particular, the ventral pallidum (VP) is closely related to regulating emotion or starting motor action in response to emotional stimuli (Singh-Bains et al., 2016). Moreover, there was a case of a patient with damage of the GP, including the VP, who reported inability to feel emotion (Vijayaraghavan, Vaidya, Humphreys, Beglinger, & Paradiso, 2008). Based on this evidence, we suggest that cardiac information is relayed to the GP (including VP), and finally, the prefrontal area has a role in initiating emotion-related behavior like facial expression or generation of feeling triggered by cardiac information processing, which is consistent with the somatic marker hypothesis. In particular, we think that information from the GP to the SFG (corresponding to the dmPFC) is more likely to be involved in the generation of feeling and information from the GP to the MFG (which corresponds to the dlPFC) and is more likely to be involved in motor action. To our knowledge, these results, especially the HEP modulation in the basal ganglia, is the first evidence that cardiac information is processed in the basal ganglia and modulated in sad face perception.

Finally, cardiac information flow from the RACC to the RMFG was decreased in sad face processing in Granger causality analysis results. The RACC, which is related not only to interoception but also to the saliency network, which processes saliency of the stimuli and converts the result between the default mode network (DMN) and the central executive network (CEN) (Goulden et al., 2014; Seeley et al., 2007). Considering that the RMFG, which corresponds to the dlPFC, is the core of the CEN, we suspect that decreased cardiac information flow from the RACC to the RMFG and increased information from the RPI to RAI to the RACC means increased conversion to the CEN and to the DMN. This is also supported by a recent study that showed that HEP processing is closely related to the DMN (Babo-Rebelo et al., 2016). Furthermore, this might be related to the cognitive decline in people with depression(Rock, Roiser, Riedel, & Blackwell, 2014).

To our knowledge, this is the first study to show different interoceptive and visual processing by the same emotional stimulus. In conclusion, our results demonstrate that processing of sad faces induces both different interoceptive information processing and visual processing compared to neutral faces, which is reflected by the HEP and VEP, respectively. Interoceptive processing involves increased bottom-up processing of the HEP from the RPI to the RAI to the RACC, while different visual processing occurs in a different area, including the visual cortical area. Additionally, we found that cardiac signals are also processed differently in the basal ganglia and prefrontal regions, and effective connectivity from the GP to the PFC is also modulated in sad face processing. We suggest that this increased connectivity reflects initiation of emotion-related behavior like facial expression or generation of feeling. Finally, RACC to RMFG connectivity, which is likely to reflect switching from the DMN to the CEN by the saliency network, was decreased.

Acknowledgement

This research was supported by the Brain Research Program through the National Research Foundation of Korea (NRF) funded by the Ministry of Science & ICT (NRF - 2016M3C7A1914448 NRF - 2017M3C7A1031331). The authors wish to acknowledge Kyung-Min An and Yong-Ho Lee for helping data acquisition.

References

Adolfi, F., Couto, B., Richter, F., Decety, J., Lopez, J., Sigman, M., . . . Ibáñez, A. (2016). Convergence of interoception, emotion, and social cognition: A twofold fMRI meta-analysis and lesion approach. *Cortex*.

Attal, Y., & Schwartz, D. (2013). Assessment of subcortical source localization using deep brain activity imaging model with minimum norm operators: a MEG study. *PLoS One, 8*(3), e59856.

Babo-Rebelo, M., Richter, C. G., & Tallon-Baudry, C. (2016). Neural responses to heartbeats in the default network encode the self in spontaneous thoughts. *Journal of Neuroscience, 36*(30), 7829-7840.

Barnett, L., & Seth, A. K. (2014). The MVGC multivariate Granger causality toolbox: a new approach to Granger-causal inference. *Journal of neuroscience methods, 223*, 50-68.

Barrett, L. F., & Simmons, W. K. (2015). Interoceptive predictions in the brain. *Nature reviews neuroscience, 16*(7), 419-429.

Batty, M., & Taylor, M. J. (2003). Early processing of the six basic facial emotional expressions. *Cognitive Brain Research, 17*(3), 613-620.

Beissner, F., Meissner, K., Bär, K.-J., & Napadow, V. (2013). The autonomic brain: an activation likelihood estimation meta-analysis for central processing of autonomic function. *Journal of Neuroscience, 33*(25), 10503-10511.

Citron, F. M., Gray, M. A., Critchley, H. D., Weekes, B. S., & Ferstl, E. C. (2014). Emotional valence and arousal affect reading in an interactive way: neuroimaging evidence for an approach-withdrawal framework. *Neuropsychologia, 56*, 79-89.

Couto, B., Adolfi, F., Velasquez, M., Mesow, M., Feinstein, J., Canales-Johnson, A., . . . Sigman, M. (2015). Heart evoked potential triggers brain responses to natural affective scenes: a preliminary study. *Autonomic Neuroscience, 193*, 132-137.

Craig, A. D., & Craig, A. (2009). How do you feel--now? The anterior insula and human awareness. *Nature reviews neuroscience, 10*(1).

Critchley, H. D., Rotshtein, P., Nagai, Y., O'doherty, J., Mathias, C. J., & Dolan, R. J. (2005). Activity in

the human brain predicting differential heart rate responses to emotional facial expressions. *Neuroimage, 24*(3), 751-762.

Damasio, A., & Carvalho, G. B. (2013). The nature of feelings: evolutionary and neurobiological origins. *Nature reviews neuroscience, 14*(2), 143-152.

Damasio, A. R. (2003). *Looking for Spinoza: Joy, sorrow, and the feeling brain*: Houghton Mifflin Harcourt.

Damasio, A. R., Grabowski, T. J., Bechara, A., Damasio, H., Ponto, L. L., Parvizi, J., & Hichwa, R. D. (2000). Subcortical and cortical brain activity during the feeling of self-generated emotions. *Nature neuroscience, 3*(10), 1049-1056.

Eckberg, D. L., & Sleight, P. (1992). *Human baroreflexes in health and disease*: Oxford University Press.

Esslen, M., Pascual-Marqui, R., Hell, D., Kochi, K., & Lehmann, D. (2004). Brain areas and time course of emotional processing. *Neuroimage, 21*(4), 1189-1203.

Fischl, B. (2012). FreeSurfer. *Neuroimage, 62*(2), 774-781.

Fukushima, H., Terasawa, Y., & Umeda, S. (2011). Association between interoception and empathy: evidence from heartbeat-evoked brain potential. *International Journal of Psychophysiology, 79*(2), 259-265.

Goulden, N., Khusnulina, A., Davis, N. J., Bracewell, R. M., Bokde, A. L., McNulty, J. P., & Mullins, P. G. (2014). The salience network is responsible for switching between the default mode network and the central executive network: replication from DCM. *Neuroimage, 99*, 180-190.

Granger, C. W. (1988). Some recent development in a concept of causality. *Journal of econometrics, 39*(1-2), 199-211.

Hämäläinen, M., Hari, R., Ilmoniemi, R. J., Knuutila, J., & Lounasmaa, O. V. (1993). Magnetoencephalography—theory, instrumentation, and applications to noninvasive studies of the working human brain. *Reviews of modern Physics, 65*(2), 413.

Harrison, N. A., Gray, M. A., Gianaros, P. J., & Critchley, H. D. (2010). The embodiment of emotional feelings in the brain. *Journal of Neuroscience, 30*(38), 12878-12884.

James, W. (1884). What is an emotion? *Mind, 9*(34), 188-205.

Liu, T.-Y., Chen, Y.-S., Hsieh, J.-C., & Chen, L.-F. (2015). Asymmetric engagement of amygdala and its gamma connectivity in early emotional face processing. *PLoS One, 10*(1), e0115677.

Luft, C. D. B., & Bhattacharya, J. (2015). Aroused with heart: Modulation of heartbeat evoked potential by arousal induction and its oscillatory correlates. *Scientific reports, 5*.

Müller, L. E., Schulz, A., Andermann, M., Gäbel, A., Gescher, D. M., Spohn, A., . . . Bertsch, K. (2015). Cortical Representation of Afferent Bodily Signals in Borderline Personality Disorder: Neural Correlates and Relationship to Emotional Dysregulation. *JAMA psychiatry, 72*(11), 1077-1086.

Maister, L., Tang, T., & Tsakiris, M. (2017). Neurobehavioral evidence of interoceptive sensitivity in early infancy. *eLife, 6*.

Oostenveld, R., Fries, P., Maris, E., & Schoffelen, J.-M. (2011). FieldTrip: open source software for advanced analysis of MEG, EEG, and invasive electrophysiological data. *Computational*

intelligence and neuroscience, 2011, 1.

Pan, J., & Tompkins, W. J. (1985). A real-time QRS detection algorithm. *IEEE transactions on biomedical engineering*(3), 230-236.

Park, H.-D., Bernasconi, F., Bello-Ruiz, J., Pfeiffer, C., Salomon, R., & Blanke, O. (2016). Transient Modulations of Neural Responses to Heartbeats Covary with Bodily Self-Consciousness. *Journal of Neuroscience, 36*(32), 8453-8460.

Park, H.-D., Bernasconi, F., Salomon, R., Tallon-Baudry, C., Spinelli, L., Seeck, M., . . . Blanke, O. (2017). Neural Sources and Underlying Mechanisms of Neural Responses to Heartbeats, and their Role in Bodily Self-consciousness: An Intracranial EEG Study. *Cerebral Cortex*, 1-14.

Park, H.-D., Correia, S., Ducorps, A., & Tallon-Baudry, C. (2014). Spontaneous fluctuations in neural responses to heartbeats predict visual detection. *Nature neuroscience, 17*(4), 612-618.

Park, J. Y., Oh, J. M., Kim, S. Y., Lee, M., Lee, C., Kim, B. R., & An, S. (2011). Korean facial expressions of emotion (KOFEE). *Seoul, Korea: Section of Affect & Neuroscience, Institute of Behavioral Science in Medicine, Yonsei University College of Medicine*.

Pollatos, O., Kirsch, W., & Schandry, R. (2005). Brain structures involved in interoceptive awareness and cardioafferent signal processing: a dipole source localization study. *Human brain mapping, 26*(1), 54-64.

Pollatos, O., & Schandry, R. (2004). Accuracy of heartbeat perception is reflected in the amplitude of the heartbeat-evoked brain potential. *Psychophysiology, 41*(3), 476-482.

Rock, P., Roiser, J., Riedel, W., & Blackwell, A. (2014). Cognitive impairment in depression: a systematic review and meta-analysis. *Psychological medicine, 44*(10), 2029-2040.

Seeley, W. W., Menon, V., Schatzberg, A. F., Keller, J., Glover, G. H., Kenna, H., . . . Greicius, M. D. (2007). Dissociable intrinsic connectivity networks for salience processing and executive control. *Journal of Neuroscience, 27*(9), 2349-2356.

Shao, S., Shen, K., Wilder-Smith, E. P., & Li, X. (2011). Effect of pain perception on the heartbeat evoked potential. *Clinical neurophysiology, 122*(9), 1838-1845.

Simmons, W. K., Rapuano, K. M., Kallman, S. J., Ingeholm, J. E., Miller, B., Gotts, S. J., . . . Martin, A. (2013). Category-specific integration of homeostatic signals in caudal but not rostral human insula. *Nature neuroscience, 16*(11), 1551-1552.

Singh-Bains, M. K., Waldvogel, H. J., & Faull, R. L. (2016). The role of the human globus pallidus in Huntington's disease. *Brain Pathology, 26*(6), 741-751.

Smith, R., & Lane, R. D. (2015). The neural basis of one's own conscious and unconscious emotional states. *Neuroscience & Biobehavioral Reviews, 57*, 1-29.

Tadel, F., Baillet, S., Mosher, J. C., Pantazis, D., & Leahy, R. M. (2011). Brainstorm: a user-friendly application for MEG/EEG analysis. *Computational intelligence and neuroscience, 2011*, 8.

Terhaar, J., Viola, F. C., Bär, K.-J., & Debener, S. (2012). Heartbeat evoked potentials mirror altered body perception in depressed patients. *Clinical neurophysiology, 123*(10), 1950-1957.

Vijayaraghavan, L., Vaidya, J. G., Humphreys, C. T., Beglinger, L. J., & Paradiso, S. (2008). Emotional and motivational changes after bilateral lesions of the globus pallidus. *Neuropsychology,*

22(3), 412.

Williams, L. M., Das, P., Liddell, B., Olivieri, G., Peduto, A., Brammer, M. J., & Gordon, E. (2005). BOLD, sweat and fears: fMRI and skin conductance distinguish facial fear signals. *Neuroreport, 16*(1), 49-52.

Experimental Paradigm

Stimulus (Sad face) 0.5s | Fixation 1s | Stimulus (Happy emoticon) 0.5s | Response block (occurs randomly) 3s

30 stimuli per each conditions in one session, total of 4 sessions

1st Epoching (VEP)
(Blue box, -700ms ~ +1300ms from onset)

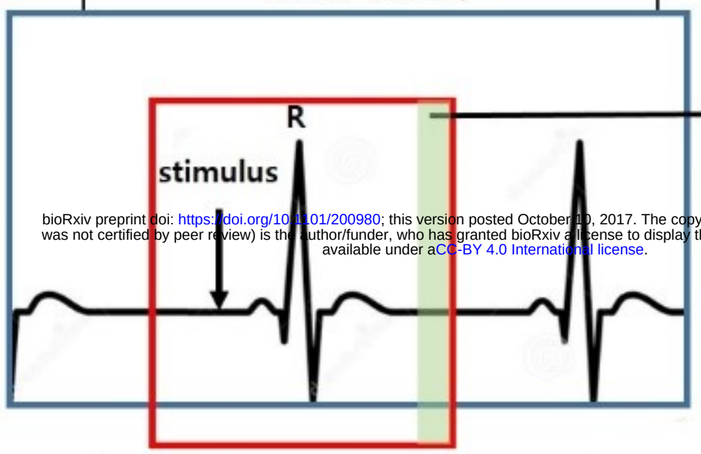

Cardiac artifact-free window (455ms ~ 595ms post R peak)

2nd Epoching (HEP)
(Red box, -500ms ~ +600ms post R peak)

Preprocessing
Artifact rejection by visual inspection
ICA correction of cardiac and eye component

Sensor level analysis → Cluster based permutation-t test between emotional and neutral condition (in cardiac artifact-free window)
Extract statistically significant sptiotemporal cluster

Source level analysis → Individual deep source modeling by Deep brain activity model and Subject T1 image data
Localize source of results in sensor analysis using statistical test in SPM12
Extract 12 ROI time courses (which have shown significant difference between conditions)

Granger causality analysis → Calculate granger causality between 12 ROIs
Calculate group-level significance of Granger causality using permutation test

Validation of HEP effect → Surrogate R peak analysis of sensor analysis results
Compare with visual evoked potential analysis results
Physiological data analysis (Heartrate, Heartbeat amplitude..)

Relationship between HEP and subjective feeling

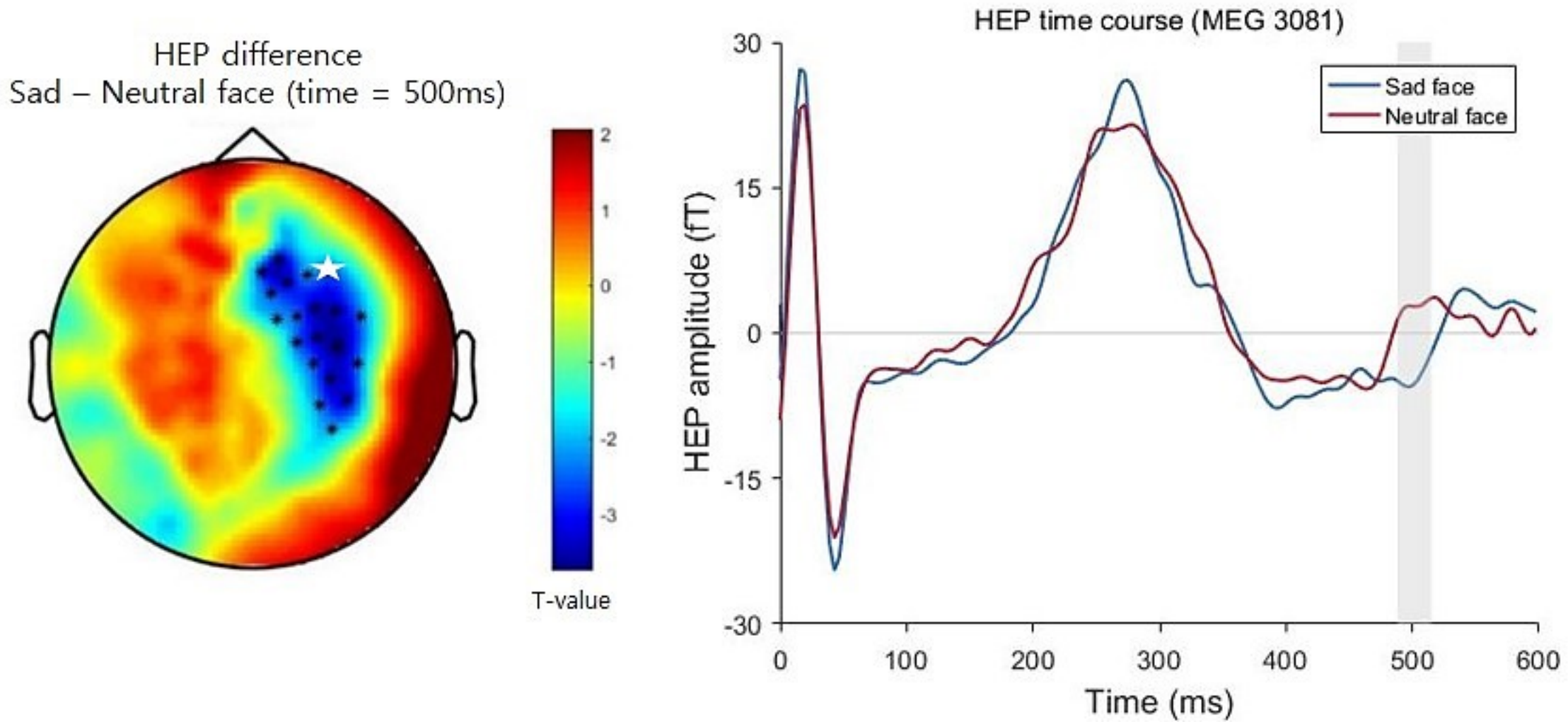
HEP difference
Sad – Neutral face (time = 500ms)
2
1
0
-1
-2
-3
T-value
HEP time course (MEG 3081)
Sad face
Neutral face
HEP amplitude (fT)
30
15
0
-15
-30
0
100
200
300
400
500
600
Time (ms)

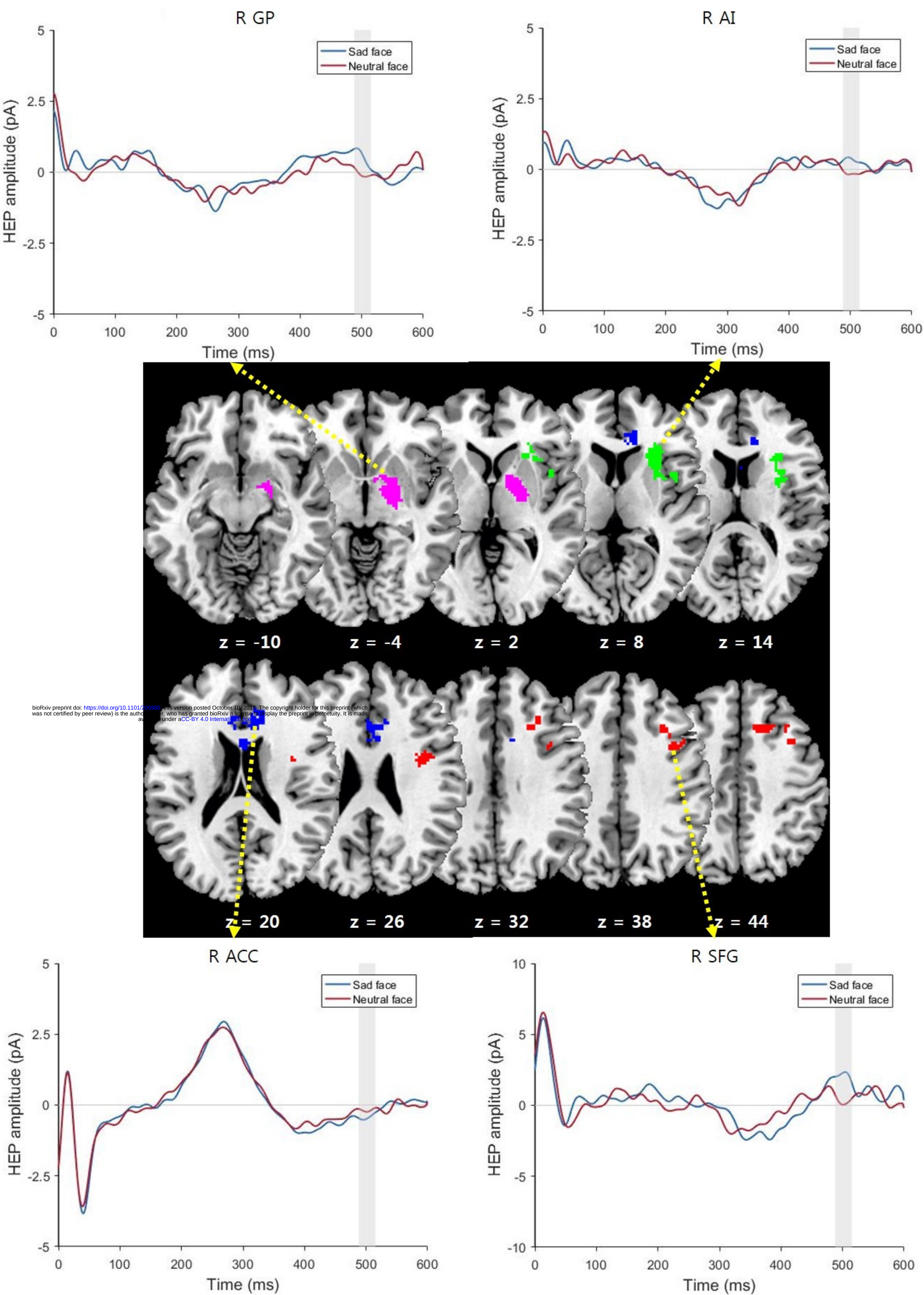

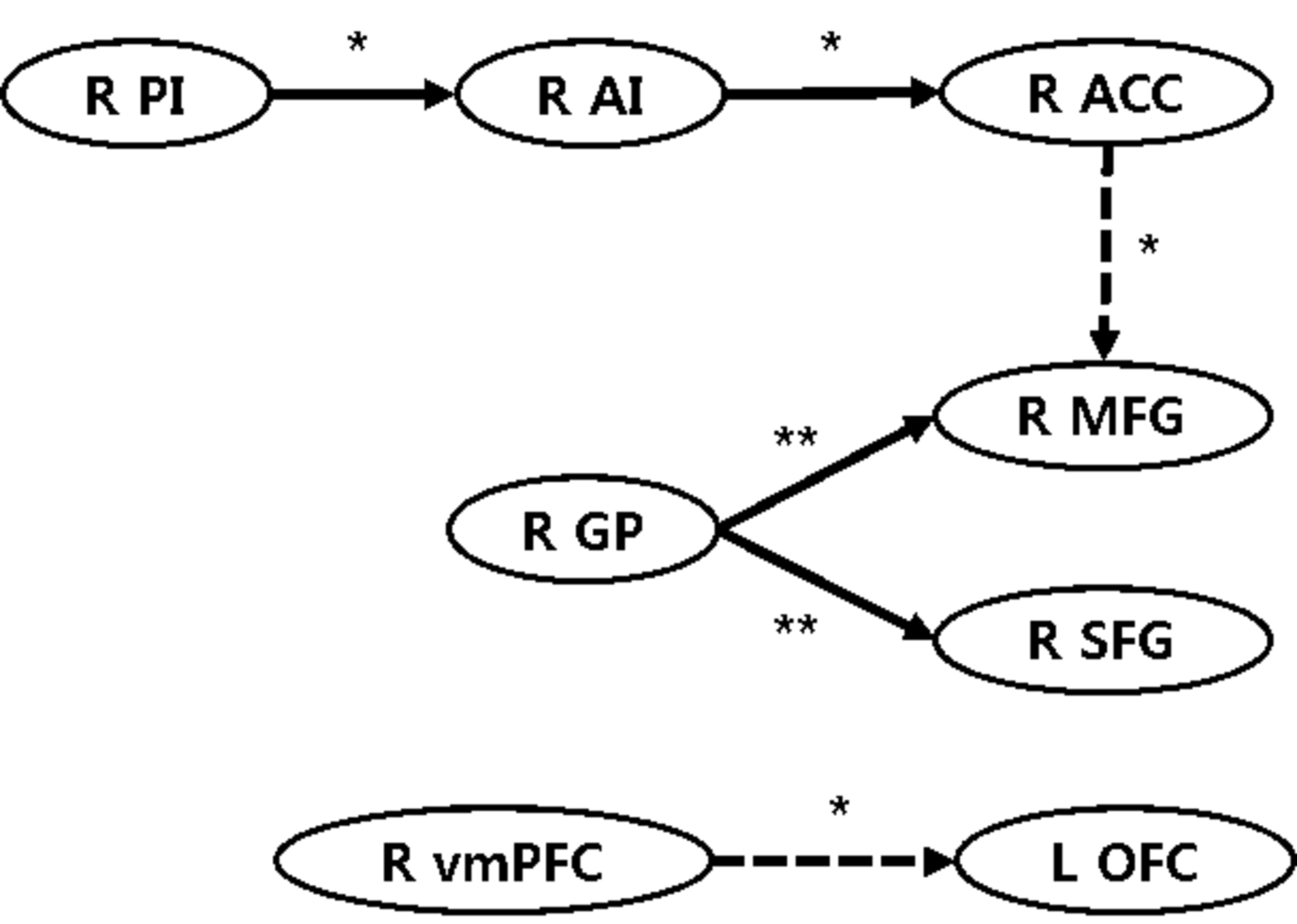
R PI
*
R AI
*
R ACC
*
R MFG
**
R GP
**
R SFG
R vmPFC
*
L OFC

a

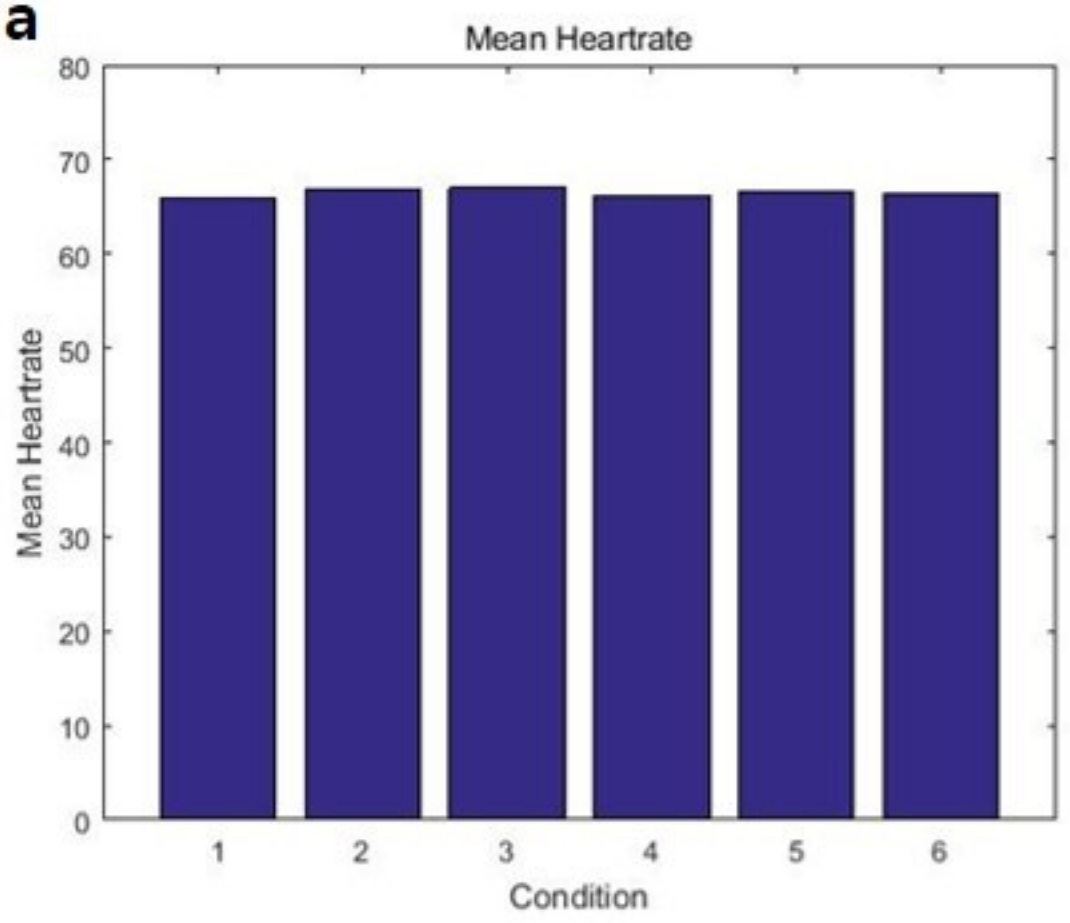
Mean Heartrate
Mean Heartrate
80
70
60
50
40
30
20
10
0
1
2
3
4
5
6
Condition

b

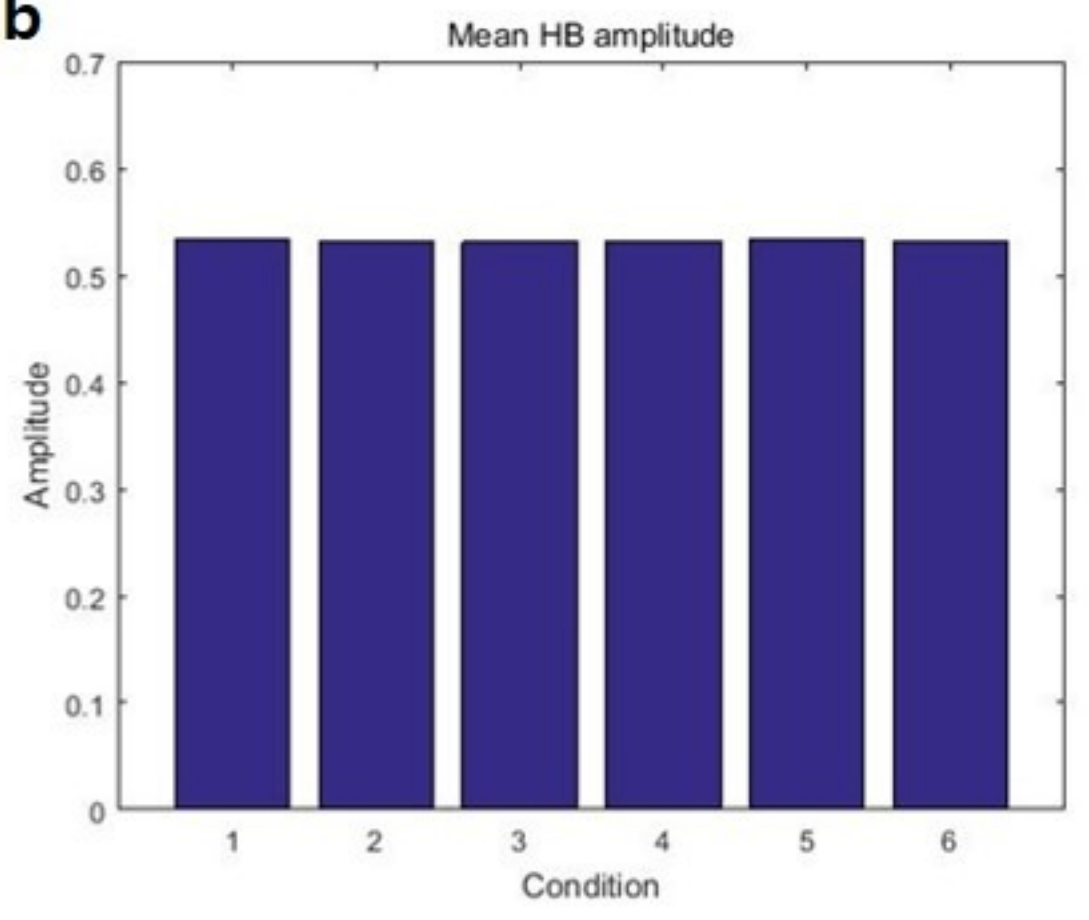
Mean HB amplitude
Amplitude
0.7
0.6
0.5
0.4
0.3
0.2
0.1
0
1
2
3
4
5
6
Condition

c

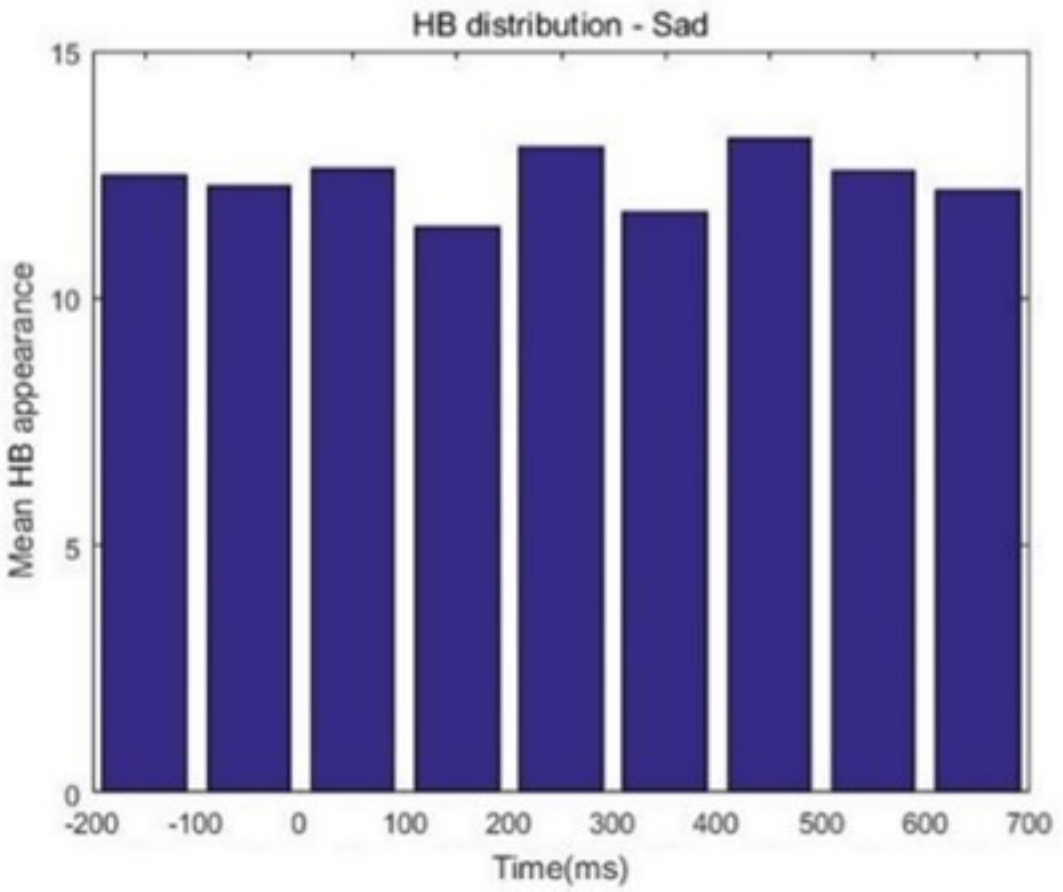
HB distribution - Sad
Mean HB appearance
15
10
5
0
-200
-100
0
100
200
300
400
500
600
700
Time(ms)

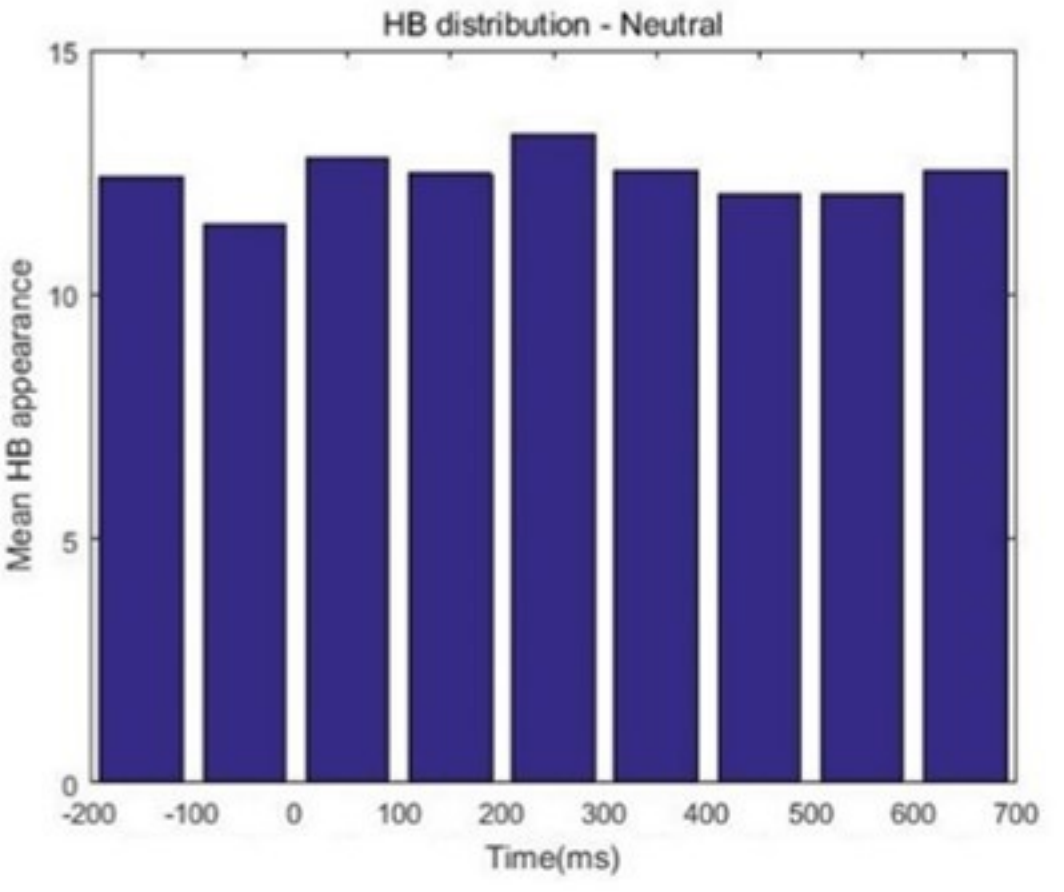
HB distribution - Neutral
Mean HB appearance
15
10
5
0
-200
-100
0
100
200
300
400
500
600
700
Time(ms)

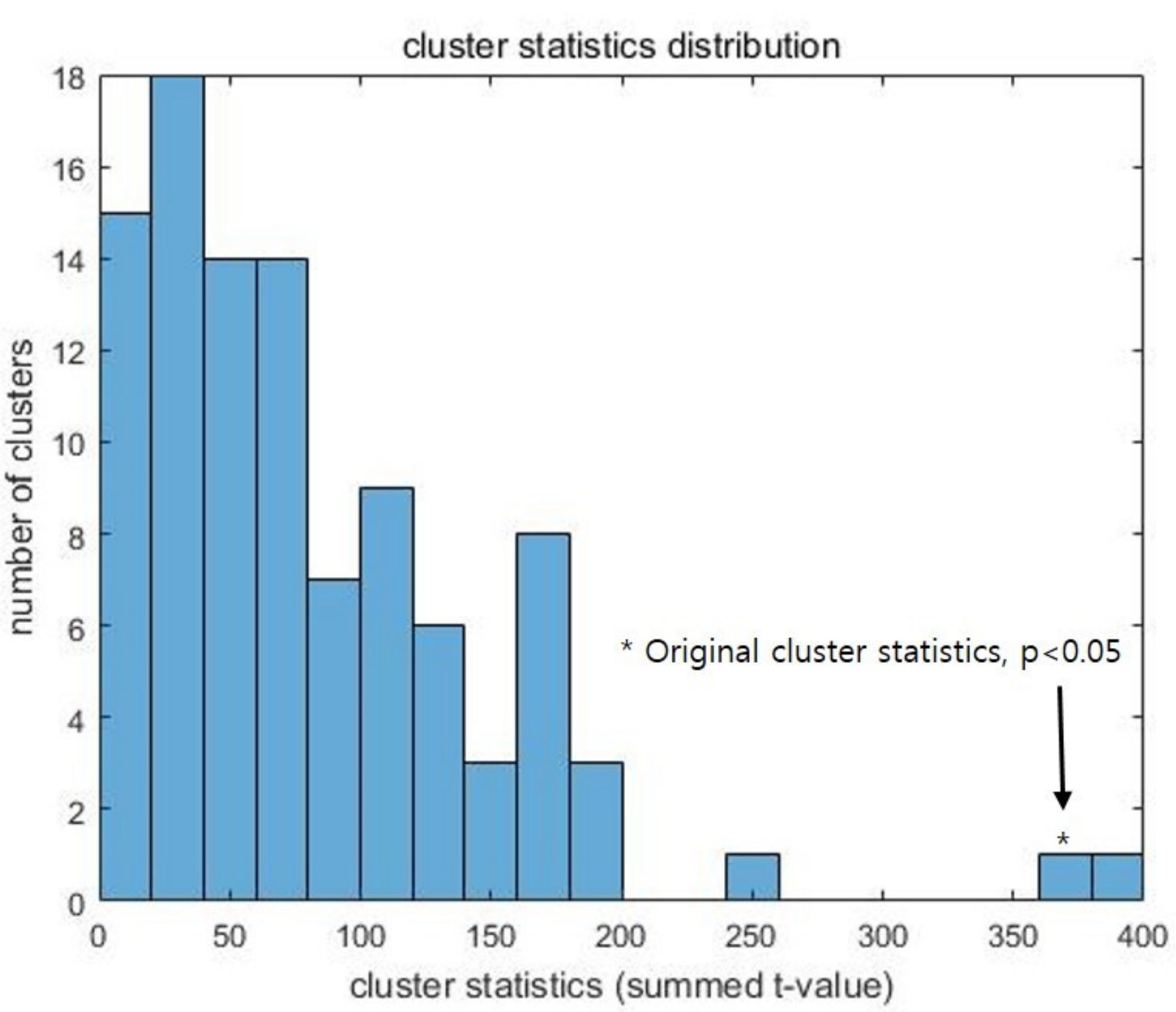
cluster statistics distribution
number of clusters
cluster statistics (summed t-value)
* Original cluster statistics, p<0.05
*
0
2
4
6
8
10
12
14
16
18
0
50
100
150
200
250
300
350
400

Regions showing VEP difference in early time range (73ms ~ 198ms)

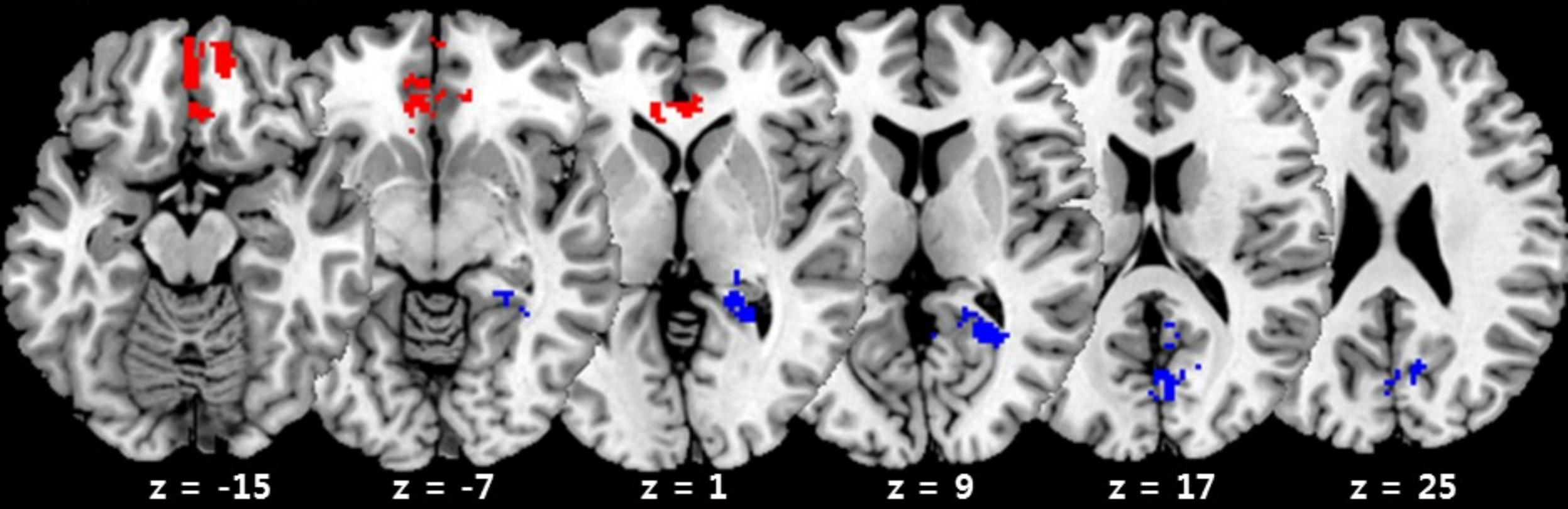

Regions showing VEP difference in late time range (815ms ~ 948ms)